Preparation of Poly(lactic acid) and Pectin Composite Films Intended for Applications in Antimicrobial Packaging

L. S. Liu,[1] V. L. Finkenstadt,[2] C.-K. Liu,[3] T. Jin,[4] M. L. Fishman,[1] K. B. Hicks[1]

[1]*Crop Conversion Science and Engineering Research Unit, Agricultural Research Service, Eastern Regional Research Center, U.S. Department of Agriculture, 600 East Mermaid Lane, Wyndmoor, Pennsylvania 19038*
[2]*Plant Polymer Research, National Center for Agricultural Utilization Research, Agricultural Research Service, U.S. Department of Agriculture, 1815 North University Street, Peoria, Illinois 61604*
[3]*Fats, Oils, and Animal Co-Products Research Unit, Agricultural Research Service, Eastern Regional Research Center, U.S. Department of Agriculture, 600 East Mermaid Lane, Wyndmoor, Pennsylvania 19038*
[4]*Food Safety Intervention Technologies Research Unit, Agricultural Research Service, Eastern Regional Research Center, U.S. Department of Agriculture, 600 East Mermaid Lane, Wyndmoor, Pennsylvania 19038*

Received 25 January 2007; accepted 6 March 2007
DOI 10.1002/app.26590
Published online 29 June 2007 in Wiley InterScience (www.interscience.wiley.com).

ABSTRACT: A pectin and poly(lactic acid) (PLA) composite was compounded by extrusion. A model antimicrobial polypeptide, nisin, was loaded into the composite by diffusion. The incorporation of pectin into PLA resulted in a heterogeneous biphasic structure, as revealed by scanning electronic microscopy, confocal laser microscopy, and fracture–acoustic emission. The incorporation of pectin also created a rough and cragged surface, which was hydrophilic and facilitated the access and absorption of nisin. The nisin-loaded composite suppressed *Lactobacillus plantarum* growth, as indicated by agar diffusion and liquid-phase culture tests. The incorporation of pectin at the concentration of $\sim$ 20% of the total mass did not alter the Young's modulus of the film from that of the pure PLA. The composite materials were able to retain their tensile strength, flexibility, and toughness to an extent that satisfied the requirements for packaging materials. Results from this research indicate the potential of pectin/PLA composites for applications in antimicrobial packaging. © 2007 Wiley Periodicals, Inc.† J Appl Polym Sci 106: 801–810, 2007

Key words: biodegradable; biopolymers; composites; extrusion; films

INTRODUCTION

New concepts and new materials for food and nonfood packaging result from flourishing manufacture and trade and are promoted by economic globalization. The global packaging market was $300 billion in 2004, and one-third of it was spent in the U.S. market. Food packaging is a large sector in the packaging industry. Among the $100 billion generated by the U.S. packaging industry, $60 billion was contributed by the food industry, and it will reach a new milestone of $74 billion by 2008.[1,2] Petroleum-derived thermoplastics with great advantages in performance and cost have dominated the packaging market to a major extent for years. Nevertheless, interests have shifted to biobased materials derived from agricultural or forestry resources because of increasing environmental concerns arising from nonbiodegradable plastics and an awareness of the limitation of petroleum resources.

Biobased materials include polysaccharides, proteins, lipids, and their polymeric extracts. They also include polymers that can be chemically synthesized from biobased monomers or produced by microorganisms or genetically modified bacteria. Poly (lactic acid) (PLA) is a biodegradable polymer made through the condensation polymerization of lactic acid. The monomer, which is also the final degradation product, can be derived through the fermentation of carbohydrate feedstocks. PLA, in the form of rigid structures, films, porous scaffolds, and micro/nanospheres, has been used for biomedical applications and disposable plastic products.[3–6] As a packaging material, PLA is attractive because it exhibits a tensile strength comparable to that of petroleum-derived thermoplastics, degrades under commercial composting conditions, and can be sealed at low temperatures. Furthermore, PLA is resistant to oil, is a good water-vapor barrier, and has relatively low gas transmittance.[7–9] PLA also has demonstrated antimicrobial activity when used in a solution of

Mention of trade names or commercial products in this article is solely for the purpose of providing specific information and does not imply recommendation or endorsement by the U.S. Department of Agriculture.

Correspondence to: L. S. Liu (linshu.liu@ars.usda.gov).

Journal of Applied Polymer Science, Vol. 106, 801–810 (2007)

oligomers or in combination with some organic acids or antimicrobial agents.[10–13] Although there are countless publications on PLA-based drug delivery systems, PLA has been less studied as an antimicrobial carrier for food and nonfood packaging. This could be imputed to its drug-release mechanism, by which the release of drugs from PLA matrices depends on PLA degradation. Another obstacle is the hydrophobic nature of PLA, to which hydrophilic antimicrobials are less accessible.

Pectin is a film-forming agent. Pectin films have shown applications in coating, encapsulating, and thickening for food and pharmaceutical uses. Pectin macromolecules bind with proteins and some organic or inorganic substances via molecular interactions. Pectin can be constructed as matrices to absorb biologically active materials and deliver the preabsorbed bioactive substances in a controlled manner.[14,15] It is expected that the incorporation of a pectin filler into a PLA matrix will result in a new complex material inheriting the advantages of the parent polymers, such as biodegradability, mechanical strength, water resistance, and accessibility to hydrophilic substances. Antimicrobial proteins can be loaded into the complex simply by a diffusion–absorption method with a higher loading efficiency and biological activity. In this article, we present a new composite material extruded from PLA and pectin. The composite was evaluated for use as a packaging material and for its antimicrobial activity after loading with an antimicrobial polypeptide, nisin.

EXPERIMENTAL

Materials

PLA was obtained from Dow Cargill (Minneapolis, MN). The weight-average and number-average molecular weights were 148,000 and 110,000; the glass-transition temperature (T_g) was 55–60°C. Nisaplin (containing 2.5% nisin) and pectin sodium salt were purchased from Danisco Cultor USA (New Century, KS); the weight-average molecular weight of pectin was 90,000, the degree of esterification was 60%, and the water content was 7.8%. Dichloromethane and acetone were from Sigma–Aldrich (Milwaukee, WI). Deionized water was prepared with a Barnstead (Dubuque, IA) E-pure water system.

Composite preparation and physical characterizations

Compounding was performed with a Werner–Pfleiderer ZSK30 corotating twin-screw extruder (Coperion Corp., Ramsey, NJ). The barrel comprised 14 sections, having a length/diameter ratio of 44 : 1. The screw configuration was reported earlier.[16] The screw speed was 130 rpm. PLA was fed into barrel section 1 with a gravimetric feeder (model 3000, AccuRate, Inc., Whitewater, WI). After the PLA was melted, pectin was fed into barrel section 7 with a loss-in-weight feeder. In all cases, the total feed rate was approximately 75 g/min. The barrel was heated with eight heating zones. The temperature profile was 135 (zone 1), 190 (zone 2), and 177°C (zones 3–8). A die plate with two holes (4 mm in diameter) was used. The melt temperature of the exudate at the die was approximately 155°C. The residence time was approximately 2.5 min. The die pressure and torque were allowed to stabilize between formulations before sample was collected. Strands were pelletized with a laboratory (2-in.) pelletizer (Killion Extruders, Inc., Cedar Grove, NJ).

Thin PLA and pectin/PLA formulations were prepared with a Brabender single-screw extruder (C.W. Brabender, South Hackensack, NJ) with four temperature zones (150, 170, 170, and 150°C). A 3 : 1 high-shear mixing zone screw was employed. Ribbons were extruded with a hangar-type die at 150°C. The thickness of the resultant materials was measured with a micrometer (Ames, Waltham, MA).

The appearance of the resultant composites was recorded with a Nikon D1x (Tokyo, Japan) camera equipped with a Nikon 100-mm macro lens. The resultant composites were characterized for the water, PLA, and pectin content by measuring the weight loss after drying and extraction with dichloromethane.[15,17] Briefly, specimens of pectin/PLA or PLA ($\sim$ 200 mg for each) were weighed, chopped into smaller pieces, placed in a 5.0-mL volumetric flask containing dry acetone, capped with a pennyhead stopper, and gently shaken at room temperature for 8 h. The acetone was refreshed three times and then pipetted out; the flask with the contents was vacuum-dried (20 μmHg) at room temperature for 24 h. The weight loss due to the drying process was considered the water content of the sample. An extraction solution of dichloromethane (5.0 mL) was added to the flask, which was gently shaken at room temperature for an additional 8 h to complete the dissolution of PLA. The extraction solution was removed, and the solid phase (pectin particles colored brown) was washed with fresh dichloromethane (3 $\times$ 5 mL) and dry ethanol (5 $\times$ 5 mL), dried under a dry N_2 jet, and weighed immediately. The weight loss due to the dichloromethane extraction reflected the amount of PLA in the composite.

The composites were cut into ASTM D 638-99 type I tensile bars (16.42 cm long $\times$ 1.91 cm wide) for the mechanical property tests, into strips (7.0 mm wide and 38.1 mm long) for the dynamic mechanical thermal analysis, and into discs (1.6 cm in diameter) for the nisin loading and antimicrobial activity assay. The bars, strips, and discs also were examined

microscopically. All sample specimens were stored in a desiccator over a desiccant at 4–7°C.

Scanning electron microscopy (SEM)

Fractured surfaces of PLA and pectin/PLA samples were examined for morphology and pectin distribution. Fractured surfaces were created either by freeze fracturing with liquid nitrogen or by separation into two parts by a destructive force during tensile testing. Sample fragments were mounted with an adhesive to specimen stubs, and the edge was painted with a colloidal silver adhesive and sputtered with a thin layer of gold. SEM images were made in a high-vacuum/secondary electron-imaging mode of a Quanta 200 FEG microscope (FEI, Hillsboro, OR). Digital images were collected at magnifications of 500, 2500, and 25000×.

Confocal laser microscopy (CLM)

For CLM, specimens were glued to a 1 cm × 3 cm microscope slide and placed on an IRBE optical microscope with a 10× lens integrated with a model TCS-SP laser scanning confocal microscope (Leica Microsystems, Exton, PA). Images were made at 633 nm for confocal reflection and at 425 nm/475 nm (excitation/emission) for autofluorescence at two channels.

Dynamic mechanical analysis (DMA)

DMA was performed on a Rheometrics (Piscataway, NJ) RSA II analyzer. The storage modulus (E') and loss modulus (E'') were measured as a function of temperature. The gap between two jaws at the beginning of each test was 23 mm; a nominal strain of 0.1% was used with an applied frequency of 10 rad/s (1.59 Hz). Each sample was equilibrated in the sample chamber under dry nitrogen at −100°C before the test was run, and the temperature was increased at the heating rate of 10°C/min; data were collected from −100 to 200°C and analyzed with Rheometric Scientific Orchestrator software (version 6.5.7).

Mechanical test and acoustic emission (AE)

The mechanical property measurements were performed with a tensile tester, which enabled us to obtain the tensile strength, Young's modulus, and toughness of the samples. The tensile strength is defined as the maximum stress to fracture composite specimens. Young's modulus is a physical quantity representing the stiffness of a material. It is determined by the measurement of the slope of a line tangent to the initial stress–strain curve from the origin to 10% strain. The toughness (also called the fracture energy) is determined by the measurement of the energy required to fracture samples, which is the area under the stress–strain curve. The properties were measured at 21°C and 65% relative humidity with a gauge length of 102 mm. An upgraded Instron mechanical property tester (model 1122) and Testworks 4 data acquisition software (MTS Systems Corp., Minneapolis, MN) were used throughout this investigation. The strain rate (crosshead speed) was set at 50 mm/min. The tensile tester was programmed to perform a cyclic test. Samples were loaded into the jaws and were then stretched to 2% strain at 50 mm/min and then back to 0% strain; once 0% strain was reached, the samples were again stretched to 2% strain and then back to 0% strain. A total of five cycles were tested, and the peak stress was recorded for each cycle.

AE measurements and tensile stress–strain tests were performed simultaneously for the samples previously described. A small piezoelectric transducer was clipped against the samples. This transducer resonated at 150 kHz (model R15, Physical Acoustics Corp., Princeton, NJ) and was 10 mm in diameter. AE signals emanating from this transducer when the Instron stretched the samples were processed with an upgraded LOCAN-AT AE analyzer (Physical Acoustics). The upgraded LOCAN-AT, which exceeded the 20-MB limit of the old LOCAN, was connected to a PC base with enhanced graphing and data acquisition software with all the features and options of the SPARTAN 2000. This AE system has been used in our research center for studying the deformation and fracture mechanisms of biocomposites, fabrics, and leather.

Nisin loading and antimicrobial activity test

Nisin was loaded into pectin/PLA and PLA through the soaking of the samples in a nisin solution. Briefly, five specimens were placed in a Petri dish (60 mm × 15 mm) containing 10.0 mL of a nisin solution (1% w/v, pH 2) and shaken at room temperature at 80 rpm for 18 h. The specimens were removed from the nisin solution and washed three times with 10 mL of 1*N* NaCl (pH 2) and three times with deionized water through the shaking of the solutions for 1 min each time. The washed sample specimens were dried in a fume hood for 30 min and stored at 4–7°C in a refrigerator before being examined for antimicrobial activity.

For the agar diffusion test, each specimen was placed on a surface-inoculated Man, Rogosa, and Sharpe (MRS) agar plate, on which 10^6 cfu/mL *Lactobacillus plantarum* was seeded. The agar plates with the specimens were incubated at 35°C for 48 h. The diameter of the growth inhibition zone was measured with a caliper. The ratio of the diameter of the

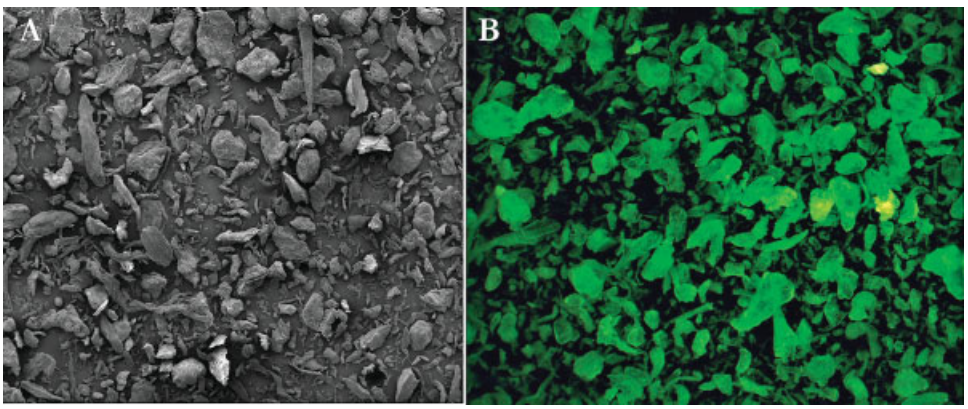

Figure 1 (A) SEM and (B) CLM images of pectin particles before extrusion. The field width was 2.6 mm. [Color figure can be viewed in the online issue, which is available at www.interscience.wiley.com.]

inhibition zone to the diameter of the specimen was used to determine the antimicrobial activity. Specimens of PLA and pectin/PLA with and without nisin loading were tested. Each sample was tested five times.

For the liquid culture test, three pieces of specimens from either a pectin/PLA composite or PLA (total surface area for each $\sim$ 12.0 cm^2) were immersed in a glass tube with 10 mL of MRS broth. The medium was inoculated with 100 μL of the *L. plantarum* culture and then was transferred to a shaker (Innovas 3100, New Brunswick Scientific, Inc., Edison, NJ) at room temperature and shaken at 200 rpm. The culture was sampled (1.0 mL) at 0, 2, 16, and 24 h. *L. plantarum* in the culture was serially diluted by a sterile phosphate buffer and then pour-plated onto MRS agar. Plates were incubated at 35°C for 48 h. A specimen-free inoculated MRS medium served as a control.

All measurements were performed on five samples, and the data were expressed as the mean plus or minus the standard deviation. The significance was determined with the use of a Student *t* test.

RESULTS AND DISCUSSION

The physical features of the pectin particles were characterized with SEM and CLM and are shown in Figure 1. The pectin particles were irregular in shape and rough in appearance and varied in size from a few micrometers to several hundred micrometers. CLM images revealed a strong autofluorescent emission colored green that outlined the shape and size of the pectin particles. The intrinsic fluorescence of pectin was used as a tool for pectin identification in pectin/PLA composite films throughout this study.

After composite compounding, PLA and pectin/PLA specimens were characterized initially for the PLA, pectin, and water contents, thickness, appearance, and surface characteristics. As shown in Table I, the composite contained $\sim$ 20% pectin and $\sim$ 7% water. The appearance of PLA and pectin/PLA composites is shown in Figure 2; the pectin particles were evenly distributed within the PLA phase. The optical transparency of the composite was inversely reduced with the addition of pectin particles [Fig. 2(A,B)]. The thin PLA and pectin/PLA composites displayed negligible changes after being bent into a circular shape, and this showed their high flexibility [Fig. 2(C,D)] as packaging materials. The surface characteristics of the composites were further identified with CLM and SEM.

Confocal fluorescence and confocal reflection microscopy were used in a correlated mode to determine the composite structure. As shown in Figure 3(A), images of reflection and fluorescence in a stereoprojection revealed an integrated structure of the two components. The reflection areas colored red contained PLA fibers. Green fluorescence images indicated an even distribution of pectin particles,

TABLE I
Components and Thickness of PLA and Pectin/PLA Composites

	Thickness (mm)	PLA content (%)	Pectin content (%)	Water content (%)
PLA	0.54 ± 0.02	100	0	<0.01
Pectin/PLA	0.55 ± 0.02	75.2 ± 3	19.1 ± 6.2	6.7 ± 1.5

The data are expressed as the mean plus or minus the standard deviation (n = 5).

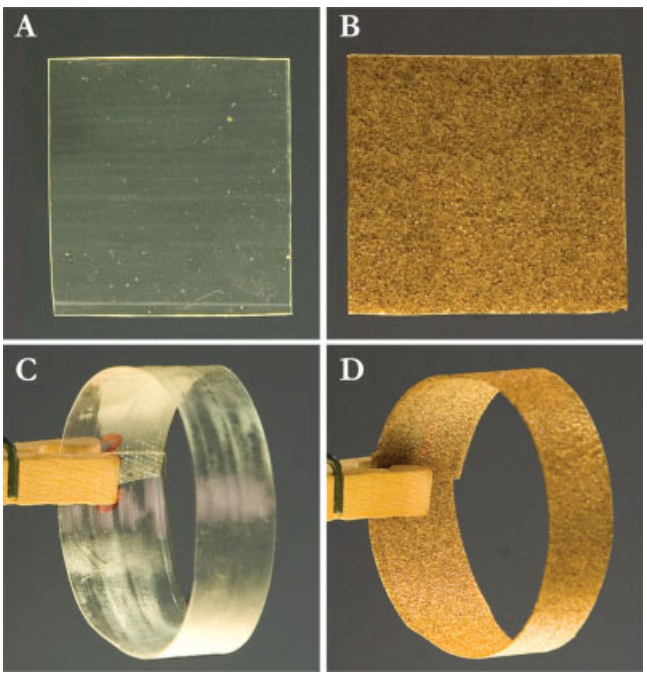

Figure 2 Photographs of (A,C) PLA samples and (B,D) pectin/PLA composites containing ~ 19% pectin particles (w/w): (A,B) top view and (C,D) side view with a circular shape. The field width was 6.0 cm. [Color figure can be viewed in the online issue, which is available at www.interscience.wiley.com.]

which was consistent with the results shown in Figure 2(B). Confocal reflection microscopy revealed a continuous, smooth surface for the pure PLA sample [Fig. 3(B)]. Confocal fluorescence indicated a discontinuous morphology for the specimens containing pectin particles. The images of the green pectin areas also revealed a relatively rough morphology, showing a cragged layer 20–30 μm thick lying on the film surfaces [Fig. 3(C)]. Furthermore, some particles were aggregated to form blocks or penetrated with PLA components [Fig. 3(A)]. This was confirmed by SEM. Figure 4(A) shows the image of a vertical section of a composite specimen. The pectin aggregates were located on the surface and extended deeply into the sample. In some areas, the pectin aggregates stretched about 300 μm below the surface, which was two-thirds of the thickness. A higher magnification showed a porous structure of pectin particles embedded in the PLA phase [Fig. 4(B)]. In comparison with the pectins before extrusion (Fig. 1), the embedded particles showed some changes in appearance, such as more porosity, containing crevices and folds. Because the composites were extruded at a high temperature and pressure, the process might have caused broken particles and/or adhesion of the particles to one another. The melted PLA also could migrate into the pectin particles. As a result, the extruded composites provided a highly porous structure consisting of pectin, which was favorable for the diffusion, adsorption, and storage of hydrophilic components. On the other hand, the reduction in the size of the PLA phase [Fig. 4(A)] could have an impact on the mechanical properties of the resultant composites. All this is discussed in detail later.

As a complement to structural studies, samples were analyzed by DMA under a small deformation force. DMA measures temperature-dependent E' and E'' values. Comparisons of typical DMA curves of PLA and pectin/PLA composites are shown in Figure 5. There was a sharp decrease in E' beginning at 54°C for both PLA and pectin/PLA composites, and this showed a T_g at about 57°C for the two films, which was consistent with the T_g of 55–60°C for PLA provided by the manufacturer. The blend of pectin with PLA did not alter the T_g value of pure PLA. This indicates the good miscibility of pectin with PLA and no chemical interactions between the two phases. Above T_g, E' of the PLA samples decreased as the temperature increased, and no response to the force could be recorded at about 120°C; this indicated that the specimen melted. For the composites, a small amount of energy was required to overcome the resistance of pectin macromolecules to thermal movement. The addition of pectin seemed to enable the composites to retain a

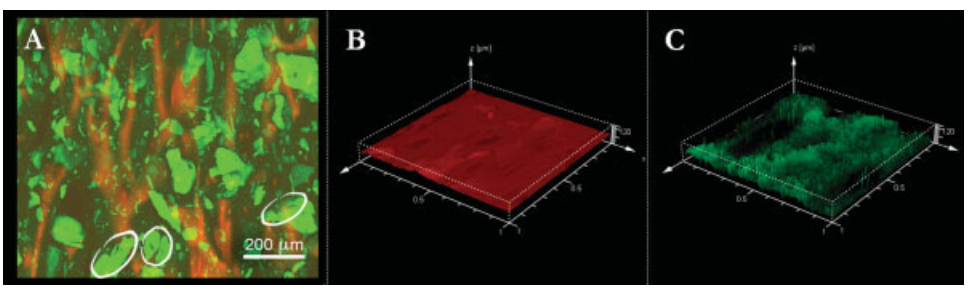

Figure 3 CLM images of (A) pectin/PLA composites by confocal reflection and confocal fluorescence in two channels, (B) pure PLA samples by confocal reflection, and (C) pectin zones by confocal autofluorescence. Areas marked by white circles in part A indicate pectin aggregation. [Color figure can be viewed in the online issue, which is available at www.interscience.wiley.com.]

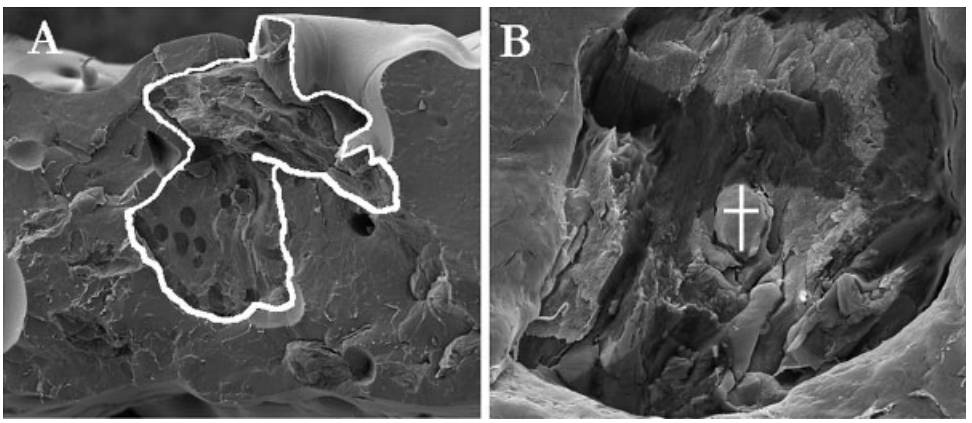

Figure 4 SEM micrographs of the composites showing that pectin particles were located on the surface and extended deep into the specimens (outlined by a white curve) and that the melted PLA penetrated the pectin aggregates (shown by a cross). The field width was (A) 530 or (B) 56 μm.

certain integrity at a higher temperature. The E'' data of PLA were similar to those of the pectin/PLA composites and showed a trend similar to that of E'.

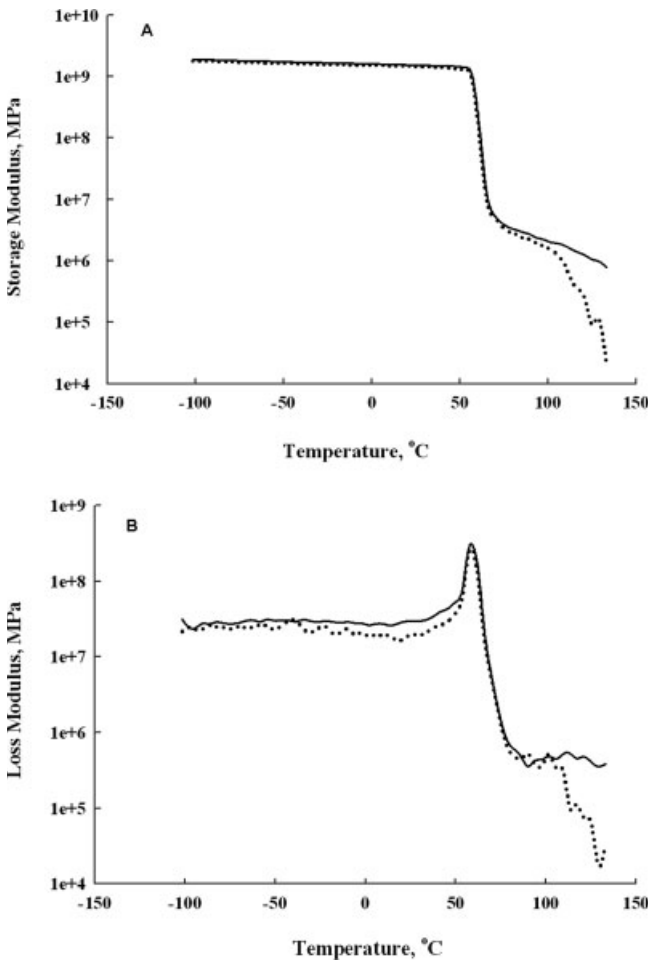

Figure 5 Typical plots of (A) E' and (B) E'' as functions of temperature. The solid line shows pectin/PLA composites; the dotted line shows PLA samples.

The samples were then subjected to a destructive analysis for mechanical resistance. AE was investigated simultaneously to collect information on structural changes during fracture. At the end of the test, the fractured surfaces of the composites were examined with SEM.

Figure 6 shows the fractured surface of the composite specimens. A clear and smooth, platelike image is evidence of the breakdown of both PLA and pectin particles under stress, indicating adhesion between the two phases. However, over all the fractured surfaces, some pectin pullout also could be observed (data not shown). A decrease in the tensile strength of about 19% and in the fracture energy of about 40% for the composite was recorded (Table II). These decreases were mainly attributed to the reduction of the PLA phase.

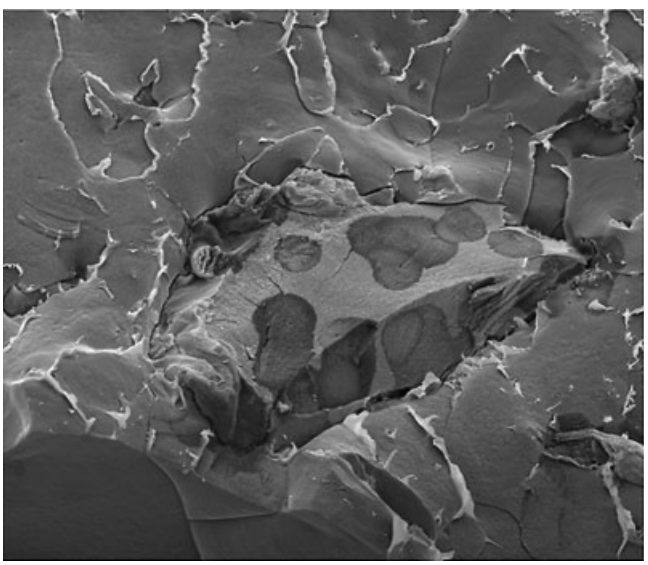

Figure 6 SEM photomicrograph of the pectin/PLA tensile fracture surface. The field width was 134 μm.

TABLE II
Mechanical Properties of PLA and PLA/Pectin Composites

Sample	Modulus (MPa)	Tensile strength (MPa)	Elongation (%)	Fracture energy (J/cm^3)
PLA	2482 ± 99	53.4 ± 3.5	3.00 ± 0.21	0.63 ± 0.11
Pectin/PLA	2598 ± 100	40.2 ± 1.1	1.98 ± 0.07	0.35 ± 0.02

The data are expressed as the mean plus or minus the standard deviation ($n = 5$, $p < 0.01$).

Figure 7 shows the correlation between the stress–strain curve and strain–AE hit rate pattern. Both PLA and pectin/PLA composites behaved as linear elastic materials. When the samples were stretched, the strain and stress increased simultaneously. For the PLA samples, the major AE activities occurred at the peak stress when the sample was completely destroyed, although a few minor AE events were also detected right before destruction, indicating the homogeneous structure of the PLA samples. The pectin/PLA composites, unlike the pure PLA samples,

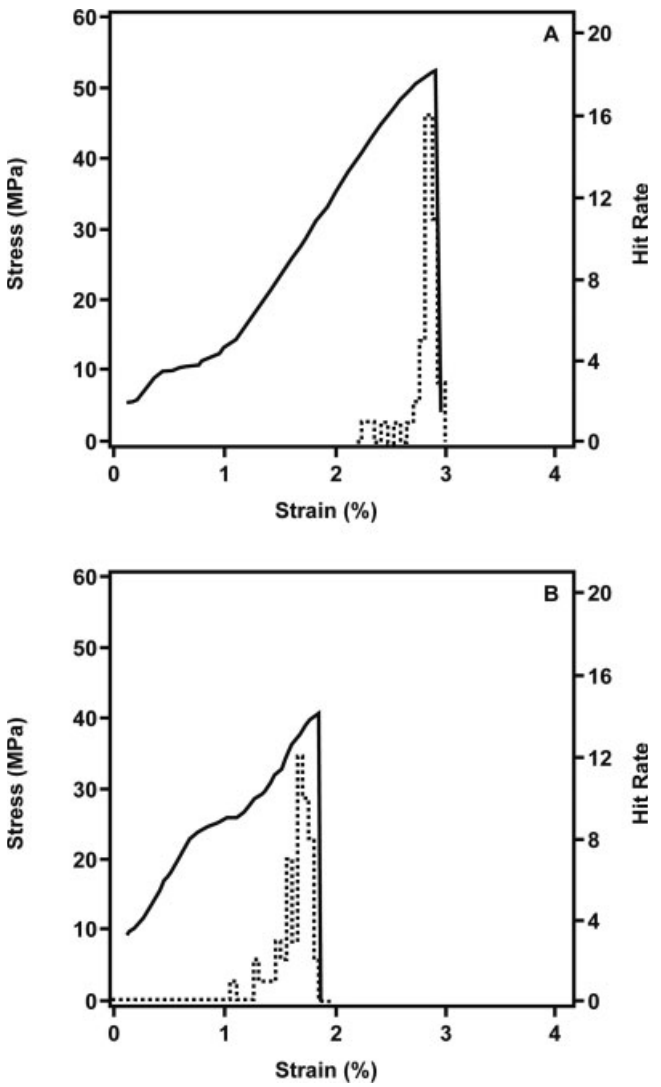

Figure 7 Correlation of the strain–stress curve (solid line) with the AE hit rate (dotted line): (A) PLA samples and (B) pectin/PLA composites.

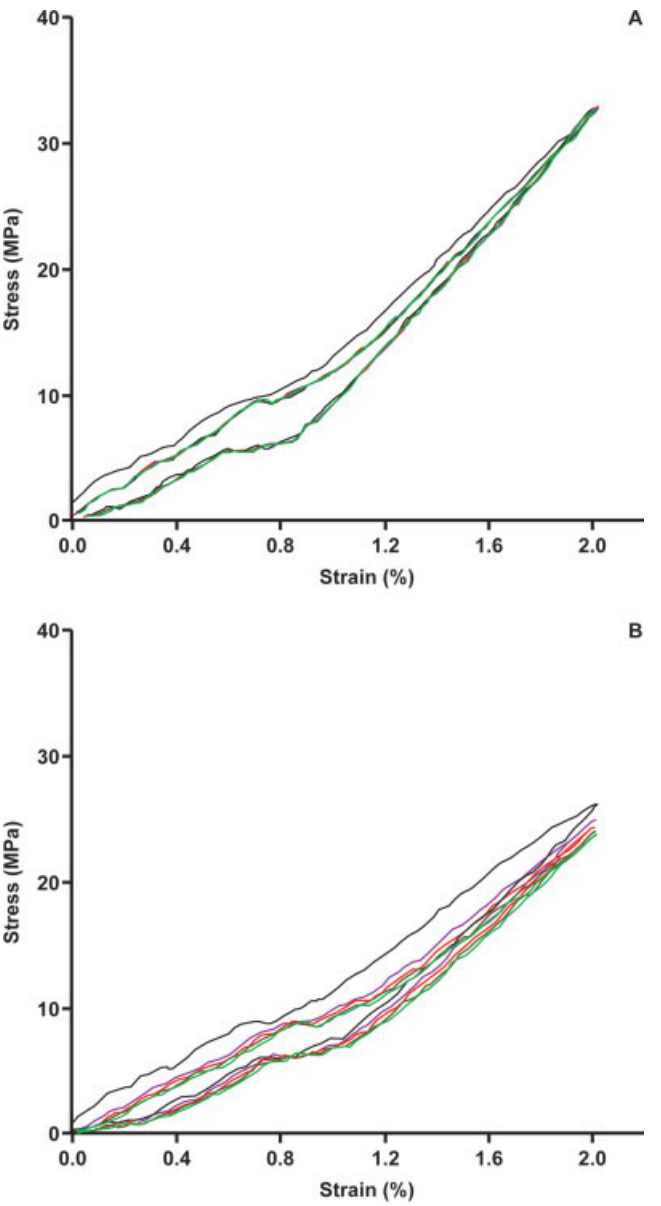

Figure 8 Stress–strain curves observed for cyclic tensile tests: (A) PLA samples and (B) pectin/PLA composites. Cycles 1–5 in sequence are colored black, purple, red, brown, and green, respectively. [Color figure can be viewed in the online issue, which is available at www.interscience.wiley.com.]

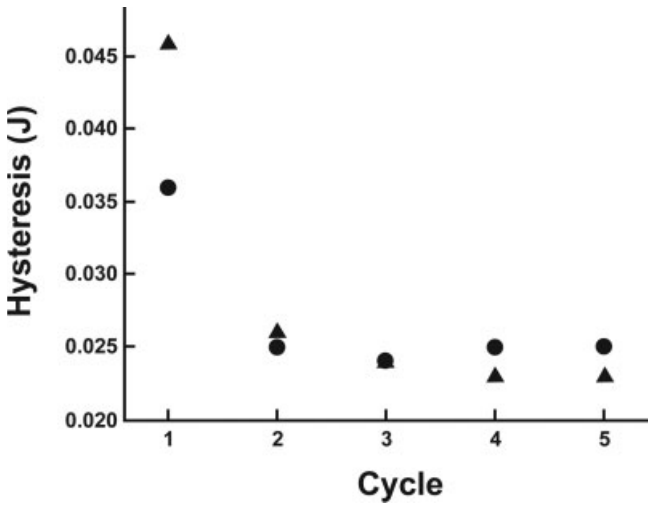

Figure 9 Energy loss (hysteresis) as a function of the cycle: (●) PLA samples and (▲) pectin/PLA composites.

emitted sound at a much earlier stretch. The early occurrence in the AE hit correlated to the increase in the slope of the stress–strain curves. This behavior indicated early defect formation probably due to separation between some pectin particles and PLA at a lower stress. The composites fractured at the maximum stress, at which the largest AE event was recorded. Such behavior is typical for a two-phase composite.

As shown in Table II, the Young's moduli of PLA and pectin/PLA were similar, ~ 2500 MPa, indicating that the two materials were similar in stiffness. To fully understand the effects of adding pectin to the PLA matrix, we also investigated the mechanical behaviors of composite samples subjected to a cyclic stretch, particularly the hysteresis, which is the energy loss during each cycle of the cycling test. It was calculated by the subtraction of the unloading energy from the loading energy. Hysteresis may have a close relationship to resiliency, which governs the dimensional stability of packaging products. Figure 8 shows the stress–strain curves as a function of the number of stretch cycles. We observed that the pure PLA samples [Fig. 8(A)] had a higher stress at loading than the pectin/PLA composite samples [Fig. 8(B)]. These stress–strain curves reveal the mechanical behavior differences between these two samples. In particular, in the first cycle, the loop (hysteresis) for the composite sample is significantly bigger than that for the pure PLA samples. Figure 9 shows the relationship between the hysteresis and stretch cycle. In the first cycle, it was evident that the hysteresis for the composite samples was greater than that of the pure PLA samples. Presumably, adding pectin to PLA led to a decrease in the elasticity of the samples, therefore increasing the hysteresis (energy loss) in cyclic tests. However, after the first cycle, there appeared to be little difference between the pure PLA and pectin/PLA composite samples. Figure 10 demonstrates the stress as a function of the stretch cycles. For the pure PLA sample, Figure 10(A) shows very little change in the peak stress, whereas Figure 10(B) clearly demonstrates that the peak stress steadily decreases as the number of stretch cycles increases. This behavior implies that the addition of pectin weakened the composites and caused more permanent deformation at the first stress; therefore, less force was needed to further stretch the sample. On the other hand, the pure PLA samples had a homogeneous structure and had a higher peak stress than the pectin/PLA composites.

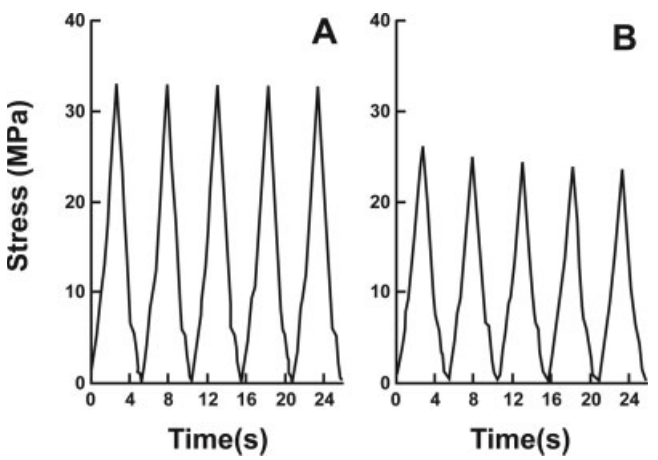

Figure 10 Stress curves as a function of time: (A) PLA samples and (B) pectin/PLA composites.

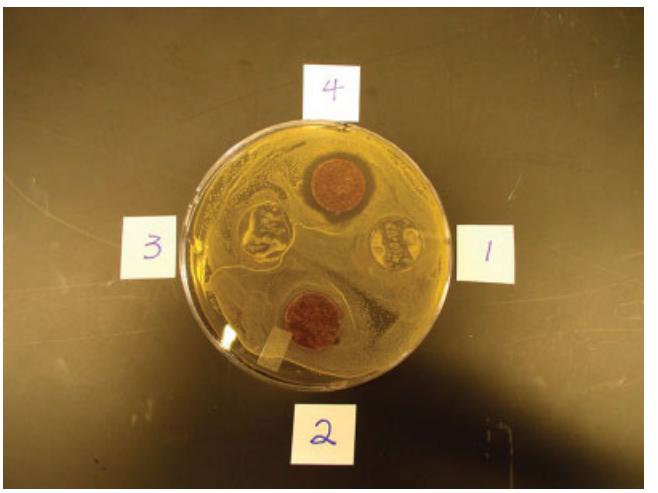

Figure 11 Antimicrobial effect on *L. Plantarum* growth by the agar diffusion method: (1,3) PLA samples and (2,4) pectin/PLA composites. Samples 1 and 2 are specimens without a nisin solution pretreatment; samples 3 and 4 are specimens with a nisin solution pretreatment. [Color figure can be viewed in the online issue, which is available at www.interscience.wiley.com.]

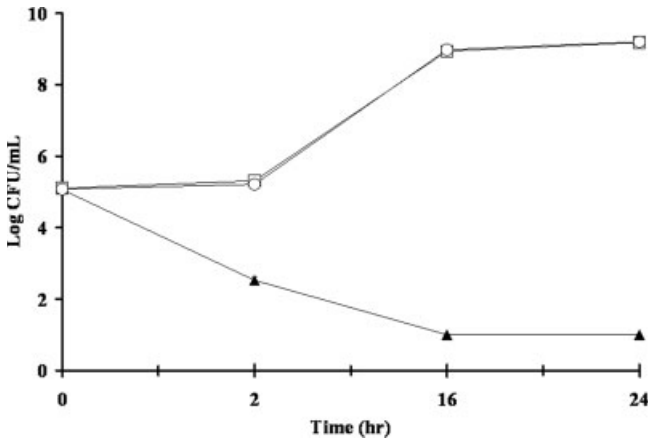

Figure 12 Antimicrobial effect on *L. Plantarum* growth by the liquid culture method: (▲) pectin/PLA composites with a nisin solution pretreatment, (○) PLA samples with a nisin solution pretreatment, and (□) a control.

This higher stress indicates that the PLA samples were structurally more resistant to deformation than the pectin/PLA composites. Because of its high resistance to deformation, the peak stress for the PLA samples remained constant through the various stretching cycles.

The inclusion of pectin reduced the tensile strength and elongation to break of PLA. Nevertheless, the pectin/PLA composites were still strong enough to serve as packaging materials if one compares their tensile strength with that of other polymeric packaging materials, such as biodegradable blends from soybean flour protein and carboxymethylated corncob (29 MPa),[17,18] nonbiodegradable poly(vinyl chloride) (35 MPa), and polystyrene (55 MPa).[19]

Samples were tested for antimicrobial activity by two methods: the agar diffusion method and the liquid-phase culture. Figure 11 shows the images taken from the agar diffusion test. Without the pretreatment of a nisin solution, PLA (sample 1) and pectin/PLA (sample 2) samples showed no antimicrobial activity. With the pretreatment of a nisin solution, PLA samples (sample 3) also showed no antimicrobial activity. This probably could be attributed to the hydrophobic nature of the PLA surfaces, which limited the nisin binding while facilitating the loss of bound nisin during the washing process. In contrast, the pectin/PLA composite samples that were pretreated with a nisin solution (sample 4) demonstrated significant antimicrobial activity against *L. plantarum*. No bacterial growth could be detected on the agar that was covered by sample 4. Furthermore, the diameter of the inhibition zone around sample 4 was 2.41 ± 0.05 cm, whereas the ratio of the diameter of the zones of inhibition to the diameter of the specimen was 1.5. This indicates that nisin was released from the composite film into the agar layer and inhibited the microbial cell growth on the agar.

To confirm this result, the samples were tested by incubation with a liquid medium containing the same bacteria under standard conditions. As shown in Figure 12, there were no differences in the microbial counts between sample 3 and the control at 0, 2, 16, and 24 h. However, sample 4 exhibited strong activity against *L. plantarum*. After 2 h of incubation, sample 4 had already reduced the cells from 5.1 logs to 2.5 logs. No colony in sample 4 was detected at a 10^{-1} dilution level (<10 cfu/mL) at 16 and 24 h, whereas sample 3 had 9 logs and 9.2 logs of the cells, respectively.

CONCLUSIONS

By the incorporation of pectin particles into a PLA matrix, we prepared a composite that could absorb and store hydrophilic antimicrobial compounds such as nisin. The resultant composite was able to inhibit bacterial growth in aqueous or gel phases by releasing the absorbed nisin. The incorporated pectin particles were located on the surface and extended deep into the materials, facilitating the access and absorption of nisin into the composites. Although the mechanical properties of the composite were somewhat poorer than those of the films made from PLA alone, they were sufficiently good to produce a viable packaging material. Further research is needed to optimize the ratio of pectin to PLA. The goal is to balance the absorption of antimicrobial reagents and the retention of mechanical properties. Furthermore, the diffusion and release kinetics of nisin into and out of the films needs to be evaluated.

The authors thank Peter H. Cooke, David Coffin, Nicholas Latona, Guoping Bao, Brian Jasberg, Rick Haig, Kathy Hornback, and Gary Grose for technical and scientific assistance.

References

1. Food Technology. http://www.itf.org. Accessed March 2006.
2. Cutter, C. N. Meat Sci 2006, 74, 131.
3. Weber, C. J.; Huagaard, V.; Festersen, R.; Bertelsen, G. Food Additives Contam 2002, 19, 172.
4. Langer, R.; Peppas, N. AIChE J 2003, 49, 2990.
5. Langer, R. Nature 1998, 392, 5.
6. Garlotta, D.; Doane, W. M.; Shogren, R. L.; Lawton, J. W.; Willett, J. L. J Appl Polym Sci 2003, 88, 1775.
7. Suyatma, N. E.; Copinet, A.; Tighzert, L.; Coma, V. J Polym Environ 2004, 12, 1.
8. Petersen, K.; Nielsen, P. V.; Bertelsen, G.; Lawther, M.; Olsen, M. B.; Nilsson, N. H.; Mortensen, G. Trends Food Sci Technol 1999, 10, 52.

9. Södergaard, A. Proceedings of the Food Biopack Conference, Copenhagen, Denmark, 2000; p 14.
10. Ariyapitipun, T.; Mustapha, A.; Clarke, A. D. J Food Prot 1999, 63, 131.
11. Alanson, A. J Food Saf 2000, 20, 13.
12. Mustapha, A.; Ariyapitipun, T.; Clarke, A. D. J Food Sci 2002, 67, 262.
13. Krishnamurthy, K.; Demirci, A.; Puri, V.; Cutter, C. N. Trans Am Soc Agric Eng 2004, 47, 1141.
14. Liu, L. S.; Cooke, P. H.; Coffin, D. R.; Fishman, M. L.; Hicks, K. B. J Appl Polym Sci 2004, 92, 1893.
15. Liu, L. S.; Won, Y. J.; Cooke, P. H.; Coffin, D. R.; Fishman, M. L.; Hicks, K. B.; Ma, P. X. Biomaterials 2004, 25, 3201.
16. Finkenstadt, V.; Liu, L. S.; Willett, J. L. J Polym Environ, to appear.
17. Liu, L. S.; Fishman, M. L.; Hicks, K. B.; Liu, C. K. J Agric Food Chem 2005, 53, 9017.
18. Schilling, C. H.; Tomasik, P.; Karpovich, D. S.; Hart, B.; Garcha, J.; Boettcher, P. T. J Polym Environ 2005, 13, 57.
19. Callister, W. D. Materials Science and Engineering, 5th ed.; Wiley: New York, 2000; p 800.